

Structural and Electrical Properties of WO_x Thin Films Deposited by Direct Current Reactive Sputtering for NO_x Gas Sensor

Young Soo Yoon, Tae Song Kim,* and Won Kook Choi**†

Department of Advanced Fusion Technology(Optical Microwave Thin Film Center), Konkuk University, Seoul 143-701, Korea

*Microsystem Research Center, Korea Institute of Science and Technology, Seoul 130-650, Korea

**Thin Film Materials Research Center, Korea Institute of Science and Technology, Seoul 130-650, Korea

(Received December 30, 2003; Accepted January 26, 2004)

ABSTRACT

WO_x -based semiconductor type thin film gas sensor was fabricated for the detection of NO_x by reactive d.c. sputtering method. The relative oxidation state of the deposited WO_x films was approximately compared by the calculation of the difference of the binding energy between O1s to $W4f_{7/2}$ core level XPS spectra in the standard WO_3 powder of known composition. As the annealing temperature increased from 500 to 800°C, relative oxygen contents and grain size of the sputtered films were gradually increased. As the results of sensitivity (R_{gas}/R_{air}) measurements for the 5 ppm NO_2 gas, the sensitivity was 110 and the sensor showed recovery time as fast as 200 s. The other sensor properties were examined in terms of surface microstructure, annealing temperature, and relative oxygen contents. These results indicated that the WO_3 thin film with well controlled structure is a good candidate for monitoring and controlling of automobile exhaust.

Key words : WO_x , Thin film, Semiconductor type sensor, NO_x , Sensitivity

1. Introduction

Nitrogen oxides NO_x (NO , NO_2) were known for not only photochemically producing ozone (O_3) that leads to create a serious metropolitan smog, but also being the cause of the acid rain destroying human ecology.¹⁾ Previously, nitrogen oxides originated from the factory and domestic heating system, but now those hazardous gases have been largely caused by the exhaust gas from the combustion engine of automobile as the use of fossil fuel is being tremendously increased.

Various kinds of NO_x sensors, such as electrochemical sensor using solid electrolyte,²⁾ superconductor type sensor based upon $YBaCu_3O_{7-x}$ thin film,³⁾ Surface Acoustic Wave (SAW) sensor⁴⁾ gas sensor using organic semiconductor like phthalocyanine,⁵⁾ and conductivity type sensor using semiconductor oxides such as SnO_2 , ZnO , WO_3 , TiO_2 ⁶⁻⁹⁾ have been widely developed. Among them, metal oxide semiconductor type gas sensors, although its sensitivity can not reach ppb level like Pb-phthalocyanine, have been much attractive for monitoring the exhaust gas from the boiler and automobile with ppm level due to durability to higher working temperature and the easy feed-back control. In the case of semiconductor type NO_x sensor, since Chang *et al.*¹⁰⁾ proposed SnO_2 -based sensor in 1979, significant results have been reported. Sbervegliri

et al.^{11,12)} reported Al, In, Cd-doped SnO_2 sensor element for NO_x sensing. Furthermore, Ishihara *et al.*¹³⁾ studied $CoO-In_2O_3$ oxide for possible application as NO_x sensing element by comparing the variations of capacitance with the change of nitrogen gas concentration. Other mixed potential type NO_x sensor using both $CdMn_2O_4$ film as a sensing part in the support of stabilized zirconia and metal oxide as a sensing electrode was also announced by Miura *et al.*¹⁴⁾ Since bulk type tungsten trioxide (WO_3) was firstly used for NO_x sensing material by Yamazoe *et al.*,¹⁵⁾ WO_3 has been known as very selective sensor material for low level concentrations of as nitrogen oxides due to its very high sensitivity.

In this study, Pt electrode was screen-printed on low-grade non-polished alumina substrate aiming at reducing the cost of mass production. Sensor element of WO_x thin films was prepared by reactive d.c. sputtering and the sensors based on those films are characterized through the analysis of the crystalline structural and electrical properties. In addition, the sensor sensitivity to NO_x gas is firstly tried to explain in terms of the nonstoichiometry, i.e. the relative oxygen to tungsten atomic ratio incorporated in the deposited films obtained by X-ray Photoelectron Spectroscopy (XPS).

2. Experimental Method

2.1. Fabrication of WO_x Sensor Element

As shown in Fig. 1, Pt electrode was screen-printed on 5 × 10 mm alumina substrate and heated at 800°C. WO_x thin film with thickness of 2 μm was sputtered on Pt/alumina

†Corresponding author : Won Kook Choi

E-mail : wkchoi@kist.re.kr

Tel : +82-2-958-5562 Fax : +82-2-958-6851

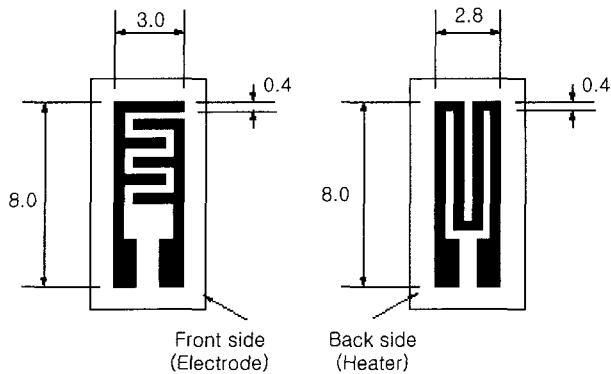


Fig. 1. Schematic diagram of the sensor structure.

Table 1. D.C. Sputtering Conditions of WO_x Thin Films

Deposition source	99.9%, 4 inch W-target
Base pressure	1×10^{-6} Torr
Deposition pressure	1×10^{-2} Torr
Sputtering gas	90%Ar : 10%O ₂
Deposition rate	5.5 Å/s
Substrate temp.	room temperature
Annealing temp. (°C)	500 – 800°C

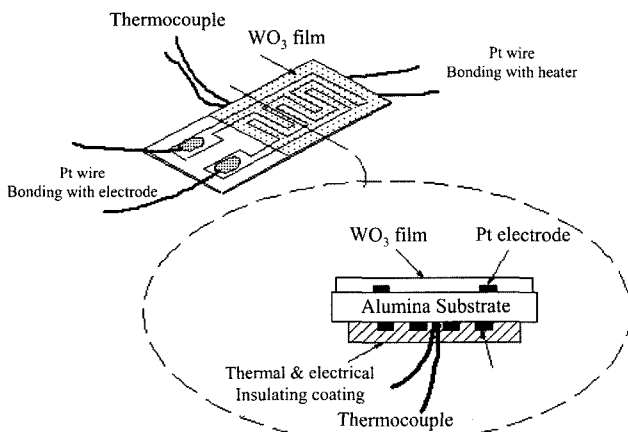


Fig. 2. Cross sectional view of NO_x sensor structure.

using pure 99.9% 4 inch W cathode and a mixture of $Ar:O_2=9:1$ plasma was used for reactive d.c sputtering. Other deposition conditions are presented in Table 1. After the deposition of WO_x thin films, these were annealed at 500 – 800°C in an air atmosphere for 4 h to enhance the oxidation and crystallization. As a heater, Pt/Au thick films (Ferro Co.) was screen-printed on the back-side and annealed at 850°C for 10 min. To monitor the working temperature, K-type thermocouple was attached at the center of the heater. The cross sectional view is shown in Fig. 2.

2.2. Measurement

The crystalline structure of sputtered WO_x sensor element thin films was analyzed by X-Ray Diffraction (XRD) using Phillips (PW 7602, Cu K_α at 30 mA and 40 kV) diffractometer. Surface microstructure of those films was examined by

Scanning Electron Microscopy (SEM; Hitachi, S-4200FE). In order to determine exactly the relative oxygen to tungsten atomic ratio in the sputtered WO_x films and the chemical shift of binding energy due to the difference in incorporated oxygen content, XPS analysis was carried out. XPS data were obtained with Al K_α radiation and all binding energy of the spectra was referenced to C1s peak at 284.6 eV. As a standard, stoichiometric WO_3 powder (Aldrich Co.) was used for the comparison of the relative oxygen to tungsten contents in the deposited films. The electrical resistance of the sensor element in air (R_{air}) and in a sample gas of NO_x (R_{gas}) was measured in $235 \times 180 \times 210 \text{ mm}^3$ closed box with an injection method. The sensitivity of the sensor element was investigated at the temperature 100 – 300°C by the Pt/Au heater using d.c 5 V input.

3. Results and Discussion

3.1. Crystalline Structure and Surface Microstructure of the WO_x Films

Fig. 3 shows XRD patterns taken from the as-deposited WO_x films and those annealed at 500 – 800°C. Around the diffraction angle of $2\theta=40^\circ$, a broad peak of W(110) plane was observed in the as-deposited film and the film appears not fully amorphous but locally crystalline structure to some extent. As the annealing temperature increased from 500 to 800°C, the deposited film showed polycrystalline WO_3 structure with the preferred orientation along $WO_3(001)$. In general, it was not easy to distinguish the XRD peaks of triclinic WO_3 from those of orthorhombic WO_3 because they had very similar diffraction angles. From the main XRD

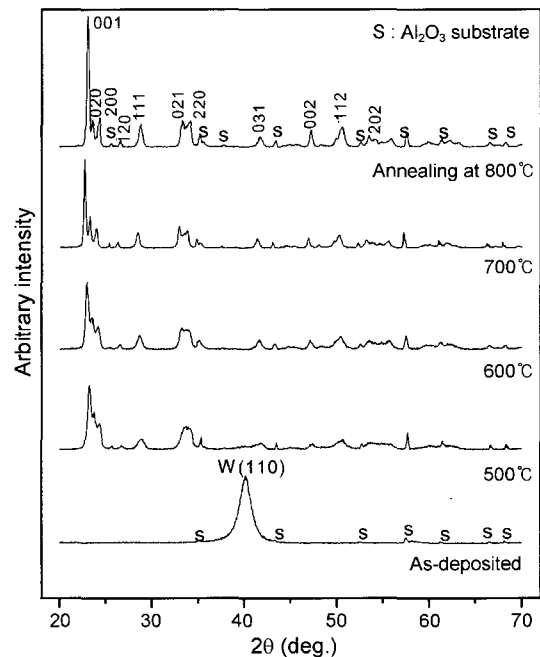


Fig. 3. XRD diffraction patterns for the sputtered WO_x thin films on alumina substrate with the variations of annealing temperature (500 – 800°C).

peak $\text{WO}_3(001)$ at $2\theta=22.5^\circ$ in Fig. 3, the annealed WO_x films were grown as polycrystalline orthorhombic structure. Fig. 4 shows SEM images of the surface microstructure of the annealed WO_x films. The as-deposited film at R.T. appeared to be covered with very small grains and sparsely huge grains as large as $1\ \mu\text{m}$ like island also consisting of a lot of small grains. As the annealing temperature increased, the size of the grains also became large and subsequently in case of the films annealed at 700°C the grain grew with the size of about $0.5\ \mu\text{m}$. This was consistent with above-mentioned XRD results indicating the sharp increase of peak intensity and reduction of the width of the main peaks as annealing temperature was increased.

3.2. X-ray Photoelectron Spectroscopy (XPS) Studies

Atomic ratios of the deposited films, ($\sigma=N_{\text{O}}/N_{\text{W}}$), were calculated by correction of $I_{\text{O}}/I_{\text{W}}$ with the observed peak area of O1s to $\text{W}4f_{7/2}$ in the standard WO_3 powder of known composition. Using the correction factor obtained from the computation of peak intensity ratio in WO_3 powder, all calculated σ 's were higher than the value of standard powder. Such an overestimation could be thought mainly because of the difference of cross section between powder particle and the solid surface. From the XPS studies, the Binding Energy (BE) shift were approximately $0.26\ \text{eV}$ for O1s and $0.61\ \text{eV}$ for $\text{W}4f$ as the relative oxygen content are increased. According to the previous article,¹⁶ it was reported that in nonstoichiometric oxide SnO_x the observed chemical shifts of the tin (Sn) cation was larger than that of oxygen anion with the increase of the oxygen content, and thus our results well agreed with the previous. According to Lau and Wertheim,¹⁷ in nonstoichiometric oxide compounds the relative shifts between O1s and the main metal core-level XPS peak was suggested to use a possible index of the oxidation stage without calibration procedures irrespective of charg-

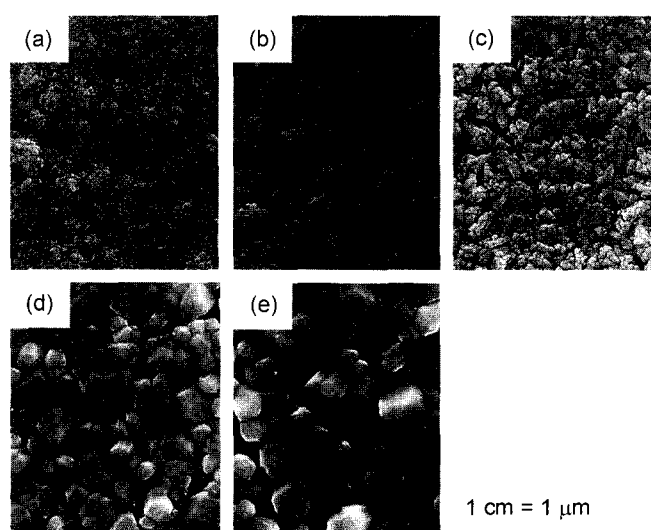


Fig. 4. SEM surface micrographs of as-sputtered WO_x film (a), and annealed at 500°C (b), 600°C (c), 700°C (d), and 800°C (e) respectively.

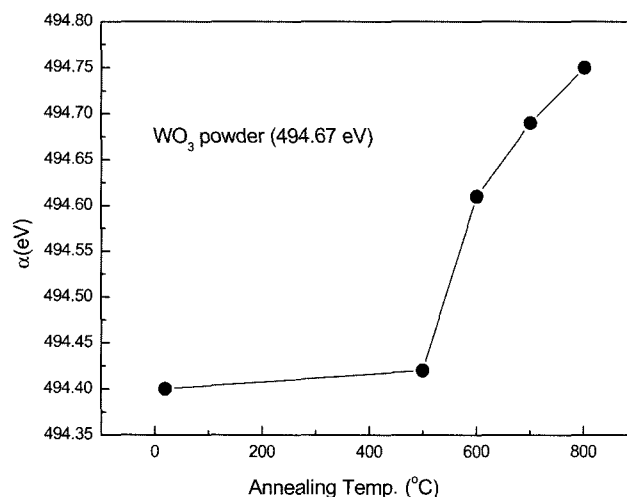


Fig. 5. XPS O1s and $\text{W}4f$ core-level spectra of the sputtered WO_x films and stoichiometric WO_3 powder (α : the binding energy difference between O1s and $\text{W}4f_{7/2}$).

ing problem in XPS. Here, the relative chemical shifts (α) between O1s and $\text{W}4f_{7/2}$ of the sputtered WO_x films were also measured to predict the oxidation state. In Fig. 5, the σ 's also increased from $494.40\ \text{eV}$ to $494.75\ \text{eV}$ as the oxygen content, i.e., oxidation state, was increased in the films. Anyway, the oxygen contents were increased as the annealing temperature increased and the films annealed at 700°C and that at 800°C were believed nearly stoichiometric or oxygen-rich WO_x .

3.3. Gas Sensitivity

To characterize WO_x -based sensor properties for NO_x gas, NO and NO_2 were used as testing gases in the concentration range of $1 - 5\ \text{ppm}$ and in the working temperature $100 - 300^\circ\text{C}$. As shown in Fig. 6, the WO_x film annealed at 600°C showed the best sensor performance with the highest sensitivity to both $5\ \text{ppm}\ \text{NO}$ ($S=21$) and NO_2 ($S=110$) gases at 200°C , respectively. Fig. 7 shows the variations sensitivity of the WO_x -based sensor annealed at 600°C with the changes of nitric oxide gases and working temperature. Below 100°C , the sensor showed low sensitivity below $S=20$. At the working temperature 200°C , it was linearly increased until $2\ \text{ppm}\ \text{NO}$ and NO_2 and greatly improved at higher concentration than $3\ \text{ppm}$. In general, the sensitivity to NO_2 gas was observed higher than that to NO gas. And then over 200°C , any response of the sensor was not found to the change of nitric oxide gas concentration.

Fig. 8 shows the characteristic behavior of the response and recovery of the sensor annealed at 600°C after $30\ \text{s}$ exposure to $5\ \text{ppm}\ \text{NO}_2$ measured at 200°C . The recovery time, defined as the time it took to reach 90% of the output voltage measured in air, was about $200\ \text{s}$. This was short compared to the recovery time of $350\ \text{s}$ taken for the reactive e-beam evaporated WO_x based sensor (not shown here). This was because the sputtered sensor element had large number of tiny reactive particles for NO_x gas to accelerate

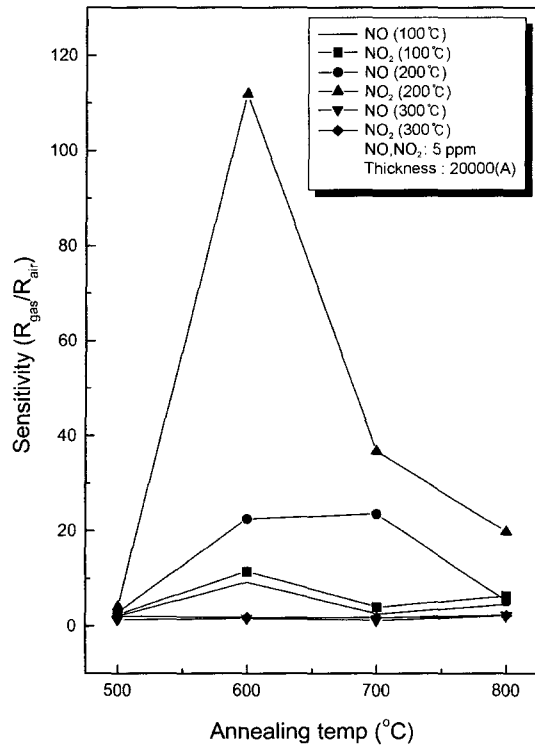


Fig. 6. Gas sensing characteristics of the WO_x thin film gas sensor annealed at 500–800°C in the working temperature 100–300°C at 5 ppm NO and NO_2 concentration.

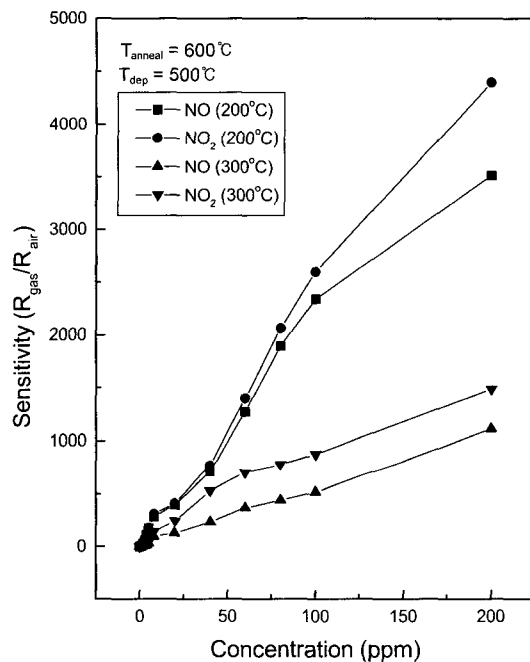


Fig. 7. Gas sensing characteristics of the WO_x thin film gas sensor annealed at 600°C as a function of NO and NO_2 concentration.

chemical reaction on the surface and thus it might directly improve the sensor properties of response and recovery behavior.

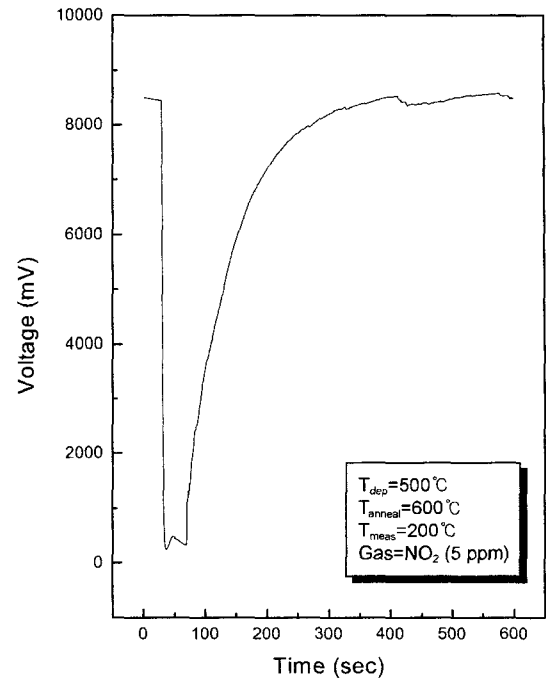


Fig. 8. NO_2 gas response time characteristics of the sensor based on the annealed WO_x film at 600°C.

4. Conclusions

The d.c sputtered WO_x films were characterized for the purpose of NO_x sensor element. As the annealing temperature in ambient environment increased, the oxygen contents were also increased. Compared to O1s and W4f BE's binding energies of standard WO_3 powder, those of the film annealed at 800°C were observed at higher positions and thus the film was believed to be oxygen-rich. Among the WO_x -based sensors, the sensor based on the film annealed at 600°C was most sensitive to NO and NO_2 gases with about $S=110$ at the annealing temperature 200°C. Even though the oxygen content and grain size of that film were smaller than those films annealed at 700 and 800°C, however, such an enhanced sensitivity of the sensor might be well explained in terms of not relative oxygen content but optimum grain size.

REFERENCES

1. H. Meixner, J. Gerblinger, U. Lampe, and M. Fleischer, "Thin-Film Gas Sensors Based on Semiconducting Metal Oxides," *Sensors and Actuators B*, **23** 119-25 (1995).
2. N. Miura, S. Yao, Y. Shimizu, and N. Yamazoe, "Development of High-Performance Solid-Electrolyte Sensors for NO and NO_x ," *Sensors and Actuators B*, **13-14** 387-90 (1993).
3. S. Kudo, H. Honishi, T. Matsumoto, and M. Ippomastu, " NO_x Sensor Using $\text{YBa}_2\text{Cu}_3\text{O}_{7-x}$ Thin Film," *Sensors and Actuators B*, **23** 219-22 (1995).
4. V. I. Anisimkin, M. Penza, A. Valentini, F. Quaranta, and L. Vasanelli, "Detection of Combustible Gases by Means of

- a ZnO-on-Si Surface Acoustic Wave (SAW) Delay Line," *Sensors and Actuators B*, **23** 197-201 (1995).
5. K. Moriya, H. Enomoto, and Y. Nakamura, "Characteristics of the Substituted Metal Phthalocyanine NO₂ Sensor," *Sensors and Actuators B*, **13-14** 412-15 (1993).
 6. I. Sayago, J. Gutierrez, L. Ares, J. I. Robla, M. C. Horrillo, J. Getino, J. Rino, and J. A. Agapito, "The Effect of Additives in Tin Oxide in the Sensitivity and Selectivity to NO_x and CO," *Sensors and Actuators B*, **26-27** 19-23 (1995).
 7. S. Matsushima, D. Ikeda, K. Kobayashi, and G. Okada, "NO₂ Gas Sensing Properties of Ga-Doped ZnO Thin Film," *Sensors and Actuators B*, **13-14** 621-22 (1993).
 8. T. Ishihara, S. Sato, and Y. Takita, "New Type NO_x Sensor Based on Capacitance Change," *Jpn. Chem. Sensors*, **9** 143-56 (1993).
 9. K. Satake, A. Katayama, H. Ohkoshi, T. Nakahara, and T. Takekuchi, "Titania NO_x Sensors for Exhaust Monitoring," *Sensors and Actuators B*, **20** 111-17 (1994).
 10. S. C. Chang, "Thin Film Semiconductor NO_x Sensor," *IEEE Trans. Electron. Devices*, **ED-26** 1875-89 (1979).
 11. G. Sberveglieri, S. Groppelli, P. Nelli, V. Lantto, H. Torvela, P. Romppainen, and S. Leppavuori, "Response to Nitric Oxide of Thin Film and Thick SnO₂ Films Containing Trivalent Additives," *Sensors and Actuators B*, **1** 79-82 (1990).
 12. G. Sberveglieri, S. Groppelli, and P. Nelli, "Highly Sensitive and Selective NO_x and NO₂ Sensor Based on Cd-Doped SnO₂ Thin Films," *Sensors and Actuators B*, **4** 457-61 (1991).
 13. T. Ishihara, H. Fujita, S. Sato, T. Fukushima, H. Nishiguchi, and Y. Takita, "Mixed Oxide of CoO-In₂O₃ as a capacitive Nitric Oxide Sensor," J. L. Baptista, J. A. Labrincha, and P. M. Vilarino (Ed.), *Electroceramics V*, Artes Graficas Servi os de Pre-Press, Portugal, 67-170, 1996.
 14. N. Miura, G. Lu, N. Yamazoe, H. Kurosawa, and M. Hasei, "Mixed Potential Type NO_x Sensor Based on Stabilized Zirconia and Oxide Electrode," *J. Electrochem. Soc.*, **143** 232-35 (1996).
 15. M. Akiyama, Z. Zhang, J. Tamaki, N. Miura, and N. Yamazoe, "Tungsten-Oxide Based Semiconductor Sensor for Detection of Nitrogen Oxides in Combustion Exhaust," *Sensors and Actuators B*, **13-14** 619-20 (1993).
 16. W. K. Choi, H.-J. Jung, and S. K. Koh, "Chemical Shifts and Optical Properties of Tin Oxide Films Grown by a Reactive Ion Assisted Deposition," *J. Vac. Sci. Tech. A*, **14** 359-66 (1996).
 17. C. L. Lau and G. K. Wertheim, "Oxidation of Tin: An ESCA Study," *J. Vac. Sci. Tech.*, **15** 622-24 (1978).